Environ Earth Sci (2014) 71:393–405
DOI 10.1007/s12665-013-2442-8

ORIGINAL ARTICLE

Radiological characterization of granitoid outcrops and dimension stones of the Variscan Corsica-Sardinia Batholith

Antonio Puccini · Gerti Xhixha · Stefano Cuccuru · Giacomo Oggiano · Merita Kaçeli Xhixha · Fabio Mantovani · Carlos Rossi Alvarez · Leonardo Casini

Received: 11 January 2013 / Accepted: 21 March 2013 / Published online: 10 April 2013

Abstract This study focuses on the radiological characterization of granitoid outcrops and dimension stones using in situ gamma-ray spectrometry. Extensive measurements were performed on 210 granitoid outcrops of the Corsica-Sardinia Batholith. The large statistical sample allowed us to improve the analysis by considering a log-normal distribution of radioelements and propagating the uncertainties using Monte Carlo method. The activity concentrations of ^{40}K, ^{226}Ra (^{238}U) and ^{232}Th in C-SB area were $1{,}177^{+408}_{-304}$, 60^{+36}_{-23} and 69^{+38}_{-25} Bq/kg (at 1σ uncertainty). The median abundance of K, U and Th on the Variscan C-SB was higher than the average values of the upper continental crust and was comparable with Variscan belt. This corresponds to an outdoor absorbed dose rate of 124^{+33}_{-26} nGy/h at 1σ uncertainty which is 3σ higher than the population-weighted average absorbed dose rate (60 nGy/h). Seven commercial granites (*Rosa Beta*, *Ghiandone*, *Giallo San Giacomo*, *Rosa Cinzia*, *Grigio Malaga*, *Bianco Sardo* and *Grigio Perla*) were investigated to characterize their radiological hazard through 147 measurements taken in 73 extractive quarries. All of the commercial granites were categorized as A2 material based on their activity concentration indices, excluding (at the 3σ level) any restriction on their utilization as superficial materials. *Rosa Beta*, *Grigio Malaga*, *Grigio Perla* and *Bianco Sardo* can also be used as bulk materials as they can be included in the A1 category. In the case of *Ghiandone*, *Giallo San Giacomo* and *Rosa Cinzia*, we are confident of an A1 classification only at the 1σ level.

Keywords In-situ gamma-ray spectrometry · Variscan Corsica-Sardinia Batholith · Granite · Dimension stones · Radiological hazard

Electronic supplementary material The online version of this article (doi:10.1007/s12665-013-2442-8) contains supplementary material, which is available to authorized users.

A. Puccini · S. Cuccuru · G. Oggiano · M. K. Xhixha · L. Casini
Department of Science of Nature and Environmental Resources, University of Sassari, Via Piandanna, 4, 07100 Sassari, Italy

G. Xhixha · F. Mantovani (✉)
Physics Department, University of Ferrara, Via Saragat, 1, 44100 Ferrara, Italy
e-mail: Mantovani@fe.infn.it

G. Xhixha
Faculty of Forestry Science, Agricultural University of Tirana, Kodër Kamëz, 1029 Tirana, Albania

G. Xhixha · F. Mantovani
Istituto Nazionale di Fisica Nucleare (INFN), Ferrara Section, Via Saragat, 1, 44100 Ferrara, Italy

C. R. Alvarez
Istituto Nazionale di Fisica Nucleare (INFN), Padova Section, Via Marzolo 8, 35131 Padua, Italy

Introduction

The gamma rays emitted from natural radioelements and, in particular, from ^{238}U and ^{232}Th decay chains and ^{40}K are important contributors to external radiation exposure. Approximately, 15 % of the world average radiation exposure comes from radioelements occurring naturally in the Earth's crust. The world average radioactivity content in the upper continental crust is 33 ± 7, 43 ± 4 and 727 ± 60 Bq/kg for ^{238}U, ^{232}Th and ^{40}K, respectively (Rudnick and Gao 2003). Materials derived from rocks and soils widely used in the construction industry may be responsible for an excess in external radiation exposure and

may also contribute to the internal radiation (owing primarily to radon and its daughters).

An enrichment of radioactivity content and, in particular, of ^{238}U and ^{232}Th in metamorphic and granitic igneous rocks is often found in a few minerals such as apatite, sphene and zircon and other accessory phases (Whitfield et al. 1959; Rogers and Ragland 1961). Igneous plutonic rocks are characterized by relatively high concentrations of natural radionuclides varying over a wide range of up to 2,000 Bq/kg for ^{40}K (Anjos et al. 2005), 600 Bq/kg for ^{238}U (^{226}Ra) (Tzortzis et al. 2003; Salas et al. 2006) and 900 Bq/kg for ^{232}Th (Tzortzis et al. 2003).

Granite production in Europe is often linked to the occurrence of several Variscan batholiths throughout the continent, from Portugal and Spain in the west to Bohemia and Poland in the east. One of the largest batholiths is the Corsica-Sardinia Batholith (C-SB) (Rossi et al. 2009), exposed in the Sardinia-Corsica Microplate. In northern Sardinia, many varieties of granitoid rocks are frequently quarried and exported throughout the world. These rocks display substantial variation in their chemical–mineralogical composition and texture, making them appealing as dimension stones for flooring, columns, ashlars and other architectural structures.

The aims of this study are

1. the realization of an extensive in situ radiometric characterization of the C-SB area using a portable scintillation gamma-ray spectrometer and the evaluation of the outdoor external dose rate;
2. the radiological characterization of commercial granite dimension stones quarried in C-SB area by adopting the activity concentration index (ACI) (EC 2011) to evaluate the radiological implications of using these rocks as building materials in dwellings.

The geochemical features of commercial granite dimension stones where discussed based on inductively coupled plasma mass spectrometry (ICP-MS) measurements. The results were cross-checked with measurements performed using a high-purity germanium (HPGe) gamma-ray spectrometer and ICP-MS.

The late Variscan granites of the Corsica-Sardinia Batholith

A large part of Sardinia, ~6,000 km^2 in total area (Ghezzo and Orsini 1982), consists of C-SB granitic rocks (Fig. 1). The C-SB is closely related to the evolution of the south European Variscan belt (Paquette et al. 2003). The C-SB formed over a time interval of approximately 60 Ma, from 340 to 280 Ma (Paquette et al. 2003; Renna et al. 2006; Gaggero et al. 2007). The long period of emplacement reflects important differences in terms of chemical composition, mineralogy and texture (Casini et al. 2012). The oldest intrusions (~340 Ma; Paquette et al. 2003) exposed in NW Corsica are represented by the so-called "durbachites" of high Mg–K calc-alkaline association. The calc-alkaline association is widespread in Sardinia and Corsica and consists mostly of metaluminous to slightly peraluminous monzogranites, granodiorites and subordinate leuco-monzogranites. The youngest magmatic bodies of calc-alkaline to transitional alkaline affinity consist of small mafic bodies, dated at approximately 285 Ma (Renna et al. 2006; Gaggero et al. 2007), that crop out in southern Corsica and Sardinia. The dominant rock types are gabbros, diorites and quartzdiorite with a tholeitic signature. Finally, in Corsica, an alkaline association of early Permian age is also documented (Cocherie et al. 2005). The Sardinian sector of the C-SB arose from the coalescence of many calc-alkaline plutons dominated by monzogranites and subordinately by granodiorites; gabbroic rocks and tonalites are very scarce (Bralia et al. 1981; Casini et al. 2012).

The dating of the calc-alkaline magmatism in Sardinia has recently been improved based on U/Pb zircon ages and Ar/Ar hornblende, muscovite and biotite ages; collectively, the data indicate a temporal window between 321 and 285 Ma (Oggiano et al. 2007; Gaggero et al. 2007). Most of the plutons emplaced between 311 and 300 Ma are mildly peraluminous monzogranites in their composition; between 300 and 285 Ma, the volume of granodiorite increased (Oggiano et al. 2005).

Three main plutons, distributed over an area of ~1,000 km^2, supply most of the granite production from Sardinia (Fig. 1c). They are, in order of importance

- the Arzachena pluton (Oggiano et al. 2005; Casini et al. 2012), which is the largest one. It shows a variety of lithofacies from almost equigranular to strongly porphyritic monzogranite (due to the occurrence of 2–3 cm-large K-feldspar phenocrysts) to equigranular granodiorites;
- the Tempio pluton (Cherchi 2005), which is comprised mostly coarse-grained biotite-rich monzogranites with huge (3–12 cm) K-feldspar xenocrysts and leuco-monzogranites;
- the Buddusò pluton (Barbey et al. 2008), characterized by an abundance of granodiorites, monzogranites and leuco-monzogranites.

The Tempio and Arzachena plutons exhibit a similar inverse zonation; the granodiorites are found in the core and progressively more differentiated terms such as monzogranites, and leuco-monzogranites are found in the outer shells. The Buddusò pluton, on the other hand, displays a normal zonation, ranging from granodioritic facies in the external shell to monzogranitic and leuco-monzogranitic facies in the core.

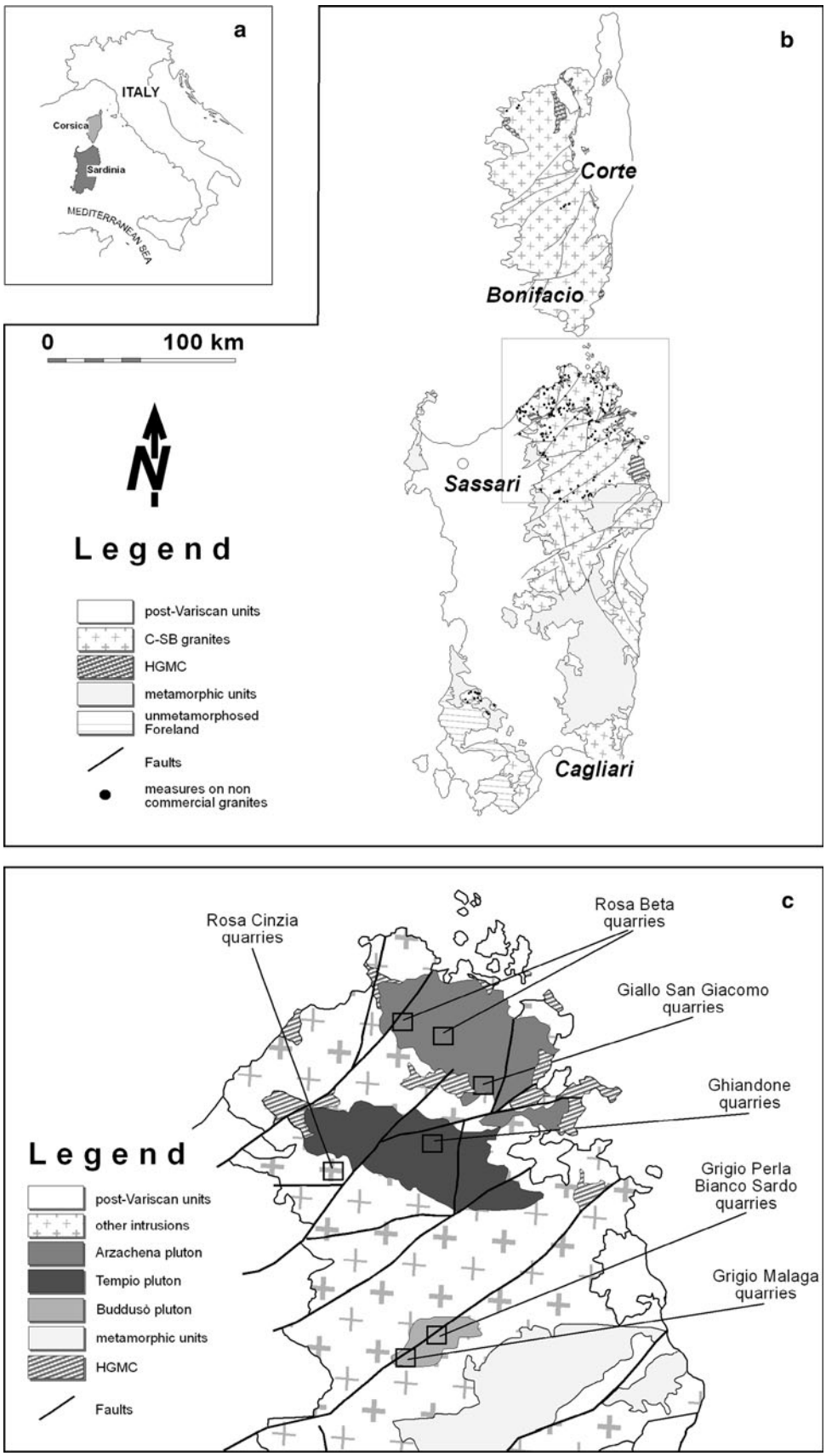

Fig. 1 **a** Position of the Corsica-Sardinia block in the Mediterranean Sea. **b** Geological sketch map of the C-SB. The 210 measurements used for its characterization are indicated by the *black circles*. **c** Position of seven extractive districts where 147 in situ measurements were performed. The Buddusò, Arzachena and Tempio plutons are also indicated. *HGMC* high grade metamorphic complex

The study of heat radiogenic elements in Sardinian sector of the C-SB is relevant for the comprehension of the origin of the extensive high-temperature and low pressure (HT-LP) province established in the Variscan belt during the Carboniferous-Permian transition. The causes of high thermal gradients which brought about anatectic melting is still debated (Cocherie et al. 1994; Faure et al. 2010). One of the hypotheses is based on a significant enrichment of heat radiogenic elements in the lower crust (Lexa et al. 2011): HT-metamorphism could be a consequence of melt-induced rheological adjustments of thick orogenic roots. The present radiological characterization of C-SB area might be included as a constraint of models which study the thermal budget of Variscan crust (Casini 2012).

Sardinian granite dimension stones and their geochemical characterization

Granites from the C-SB have been utilized extensively since ancient times (Poggi and Lazzarini 2005) and are still exploited from approximately 400 quarries in Northeast Sardinia (RAS 2007) and traded worldwide (Fig. 1c). The dimension stones are appreciated by the market as both structural (concrete, masonries, columns, etc.) and ornamental components (flooring, tiles, boards, etc.). The most famous granites[1] from C-SB are known commercially as *Rosa Beta*, *Ghiandone*, *Giallo San Giacomo*, *Rosa Cinzia*, *Grigio Malaga*, *Bianco Sardo* and *Grigio Perla*.

Rosa Beta (Fig. 2a) and *Giallo San Giacomo* (Fig. 2c) are the two commercial granites exploited from the Arzachena pluton (Fig. 1c). *Rosa Beta* is the most commercialized biotite-monzogranite among the Sardinian granites (RAS 2007). This pinkish rock has a medium grain size ranging from 0.5 to 2 cm and a strong porphyritic fabric owing to the presence of K-feldspar phenocrysts (2–3 cm). *Giallo San Giacomo* is a biotitic leucomonzogranite with an apparently isotropic and almost equigranular fabric; this granite is highly valued in the current market for its typically yellowish hue, arising from selective weathering and oxidation of Fe–Mg minerals (Cuccuru et al. 2012).

Ghiandone (Fig. 2b) is found in the Tempio pluton (Cherchi 2005) and was the most widely traded granite in the 1970s and 1980s (RAS 2007). It is a coarse-grained, strongly porphyritic biotite-monzogranite with large K-feldspar phenocrysts (up to 12 cm) dispersed within a finer-grained matrix (0.5–2 cm) composed of K-feldspar, quartz and plagioclase. *Rosa Cinzia* (Fig. 2d) is a pinkish, nearly equigranular biotite-monzogranite exploited in only three quarries located around the town of Tempio Pausania. Its grain size ranges from 0.5 to $\sim$1.5 cm, which is finer than that of *Rosa Beta*.

Grigio Malaga (Fig. 2e), *Grigio Perla* (Fig. 2f) and *Bianco Sardo* (Fig. 2g) are the three commercial granites exploited in the Buddusò pluton and represent the least, intermediate and most differentiated terms of the Buddusò intrusion, respectively (Barbey et al. 2008). *Grigio Malaga* is a tonalitic granodiorite with a grain size between 0.5 and 1.5 cm. This stone displays a well-foliated fabric that is revealed by the shape preferred orientation of its mafic enclaves and its amphibole-biotite-rich domains. *Grigio Perla* is a biotite-monzogranite with a grain size of approximately 1 cm and a gray, nearly equigranular fabric. *Bianco Sardo* is a leuco-monzogranite characterized by an equigranular fabric, relatively fine grain size ($\sim$1 cm) and overall whitish color owing to a scarcity of biotites.

The geochemical characterization is obtained from ICP-MS analysis of representative samples, which are ordered in Table 1 according to silica content. The SiO_2 content of samples ranges from 68.8 % in *Grigio Malaga* to 77.6 % in *Giallo San Giacomo*. The A/CNK ratio[2] generally increases with the silica content, varying from 0.96 in *Rosa Beta* up to 1.04 in *Giallo San Giacomo*. This indicates that all granites are metaluminous to slightly peraluminous, as commonly observed in most granites of the C-SB (Casini et al. 2012; Barbey et al. 2008).

The abundances of Ba and Sr show a negative correlation with the SiO_2 content. This behavior is even more apparent for other trace elements at the scale of a single pluton such as Buddusò pluton (*Grigio Malaga*, *Grigio Perla* and *Bianco Sardo*). The chondrite-normalized rare earth element (REE) contents are consistent in all samples (Fig. 3) showing almost flat heavy REE patterns and moderately enriched light REE, which indicates slight fractionation ($Ce/Yb = 8 \div 10$). All samples are characterized by a negative Eu anomaly, which increases from relatively basic (*Grigio Malaga*) to the more acidic materials (*Bianco Sardo*, *Giallo San Giacomo*) (Fig. 3). These observations suggest that all of the investigated granites derived from a common crustal source, as already proposed by Ferrè and Leake (2001).

The high radioactivity content in igneous rocks is generally attributed to the enrichment of U and Th. Uranium phases such as uraninite, beta- and alpha-uranophane and thorium phases such as thorianite have occasionally been identified only in pegmatites and similar highly evolved magmatic liquids (Gamboni and Gamboni 2006). Although these bodies may be common in the apical part of any intrusions (e.g., the Arzachena Pluton (Cuccuru et al. 2011)), their volume and consequently their contribution to

[1] The names of granite dimension stones are taken from UNI EN 12440 (2008).

[2] The ratio of aluminum/total alkali content is obtained by $Al_2O_3/(CaO + Na_2O + K_2O)$.

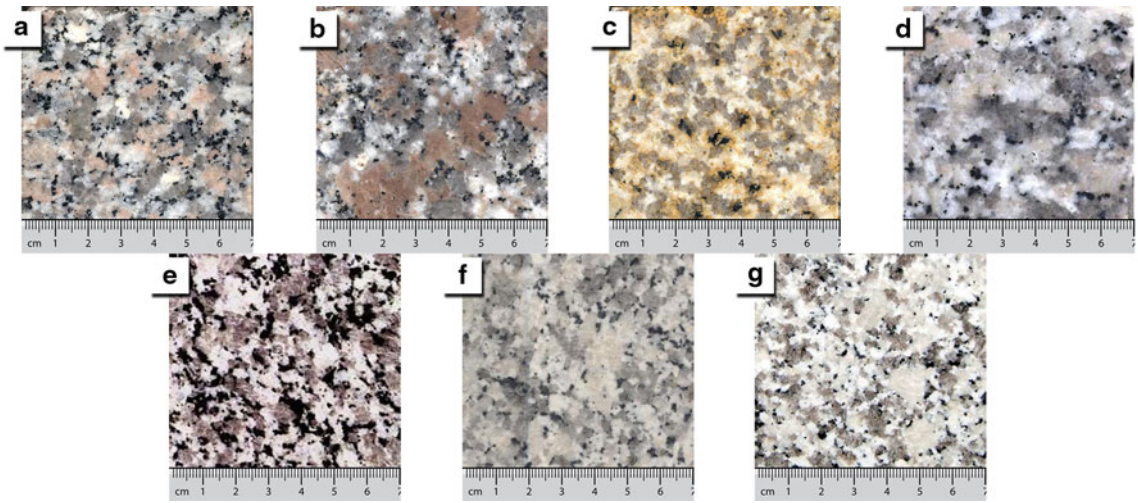

Fig. 2 Seven commercial granite tiles of **a** *Rosa Beta*, **b** *Ghiandone*, **c** *Giallo San Giacomo*, **d** *Rosa Cinzia*, **e** *Grigio Malaga*, **f** *Grigio Perla* and **g** *Bianco Sardo*

the bulk radioactivity are generally negligible. However, most granites contain a significant (1–2 wt%) quantity of U and Th bearing accessory mineral phases, such as zircon, allanite, apatite, monazite and xenotime (Gamboni and Gamboni 2006).

In our samples, the general increase of U and Th observed in the more evolved granites ($SiO_2 > 70$ wt%) correlates well with a decrease in the ZrO_2 component and increase of Y. This indicates that zircon is probably the main U and Th bearing mineral in the less evolved samples such as *Rosa Beta*, *Ghiandone* and *Grigio Malaga*, while Y-bearing phases such as allanite and xenotime become progressively more important during the evolution of magmas.

Materials and methods

In this study, a total of 357 in situ gamma-ray measurements were performed. Of these, 210 were measured on granitoid outcrops of the C-SB (Fig. 1b) and 147 were measured on 73 quarries of *Rosa Beta*, *Ghiandone*, *Giallo San Giacomo*, *Rosa Cinzia*, *Grigio Malaga*, *Bianco Sardo* and *Grigio Perla*, collecting for each lithotype 21 measurements (Table A.1).

A portable equipment mounted in a backpack and enfolded in shock-resistant materials to prevent damage in outdoor environments was used. The scintillation gamma-ray spectrometer inside the backpack consisted of an NaI(Tl) crystal with a cubic shape ($10.2 \times 10.2 \times 10.2$ cm^3) and an energy resolution of 7.3 % at 662 keV (^{137}Cs) and 5.2 % at 1,172 and 1,332 keV (^{60}Co). The crystal was optically coupled to a photomultiplier tube with integrated electronics consisting of a bias supply, preamplifier and digital multichannel analyzer (MCA). The system was managed using a notebook computer fitted with a GPS antenna (54 channels and 10 m accuracy).

The instrument was carefully calibrated following the method described in Caciolli et al. (2012). Using full spectrum analysis with the non-negative least squares (FSA-NNLS) constraint, each measured spectrum is reconstructed from a linear combination of standard spectra for ^{238}U, ^{232}Th, ^{40}K, ^{137}Cs and background. The systematic uncertainty of the method is estimated to be 5 % for ^{40}K and 7 % for ^{232}Th. The primary contributor to the U standard spectrum is the decay of ^{214}Bi, a daughter of ^{222}Rn, which is present in the ground and in the air. Although the instrument cannot discriminate between the two contributions from the ground and the air, the systematic uncertainty in the ^{238}U measurement for the ground is of order 15 % (Caciolli et al. 2012). In the case of 5-min in situ measurements on C-SB outcrops, the statistical uncertainties were <1.5, 3 and 3 % for ^{40}K, ^{238}U and ^{232}Th, respectively (Table A.1).

The main advantages of using in situ measurements are (a) quick feedback, (b) a large sample size, (c) immediate repeatability of the measurement and (d) low management costs. In contrast to laboratory HPGe spectrometry and ICP-MS, in situ gamma-ray spectroscopy provides a direct measurement of the radioactivity content of a large portion of rock. In our study, 357 in situ measurements were performed with the detector on the ground. In this configuration, 90 % of the signal reaching the detector came from a volume of radius 35 cm and ~20 cm thick, corresponding to an effective rock mass of ~200 kg.

A number of relevant precautions were taken to ensure the reliability of our measurements. To minimize the interference due to morphology, relatively flat outcrops

Table 1 Whole-rock major (wt %) and trace (μg/g) element compositions of the 7 commercial granites. Conservatively, an accuracy of 10 % for ICP-MS results was assumed

Chemical composition	Commercial granites						
	Grigio Malaga Sa15[a]	Rosa Beta	Grigio Perla	Ghiandone	Rosa Cinzia	Bianco Sardo Sa22c[a]	San Giacomo
Major elements (expressed in wt%)							
SiO_2	68.75	71.11	72.43	73.02	74.31	75.09	77.59
Al_2O_3	15.28	13.85	14.02	13.35	13.41	13.48	12.18
Fe_2O_3	3.81	0.8	0.62	1.18	0.69	1.42	0.78
FeO	–	1.82	1.46	1.09	0.93	–	0.29
CaO	3.34	2.33	1.84	2.46	1.75	1.52	0.57
Na_2O	3	3.57	3.38	3.2	3.15	3.07	3.34
K_2O	3.72	3.91	4.37	3.22	4.62	4.81	4.74
MgO	0.92	0.71	0.44	0.75	0.29	0.24	0.05
TiO_2	0.4	0.353	0.187	0.295	0.163	0.09	0.06
P_2O_5	0.15	0.34	0.06	0.09	0.04	0.07	0.03
MnO	0.05	0.065	0.082	0.065	0.033	0.04	0.02
LOI	0.5	0.72	0.54	0.62	0.44	0.59	0.28
Total	**99.92**	**99.78**	**99.59**	**99.46**	**99.93**	**100.42**	**99.95**
Trace elements (expressed in μg/g)							
Be	–	3	2	2	2	–	1
Sc	–	7	6	5	3	–	2
V	43	33	14	36	13	6	<5
Cr	10	<20	<20	<20	<20	–	40
Co	5	3	2	3	1	1	<1
Ni	–	<20	<20	<20	<20	–	<20
Cu	–	< 10	< 10	20	< 10	–	<10
Zn	57	<30	50	50	<30	25	<30
Ga	19	16	17	16	15	15	18
Ge	–	1	2	2	2	–	1
As	–	<5	<5	<5	<5	–	<5
Rb	108	120	165	112	139	123	101
Sr	195	211	88	171	93	70	13
Y	17	23	38	15	16	11	29
Zr	177	251	115	113	107	25	269
Nb	9	13	13	10	9	6	6
Mo	–	<2	<2	<2	<2	–	4
Ag	–	1.1	<0.5	<0.5	<0.5	–	<0.5
In	–	<0.2	<0.2	<0.2	<0.2	–	<0.2
Sn	–	4	5	3	3	–	4
Sb	–	<0.5	<0.5	<0.5	<0.5	–	<0.5
Cs	4	3	3	2.7	2.9	2	1.1
Ba	1,197	888	465	470	507	285	189
La	49.9	38.6	26.6	24.9	26.9	17	32.6
Ce	95.2	74.8	54	48.3	54	37.5	73.5
Pr	10.56	8.13	6.5	5.46	6.28	4.51	7.82
Nd	36.8	28.8	24.7	20.1	23	15.9	27.7
Sm	6.06	5.6	5.5	3.5	4.1	3.09	5.3
Eu	1.23	1.08	0.57	0.69	0.67	0.49	0.21
Gd	3.88	4.6	5	2.7	3.1	2.28	4.7
Tb	0.6	0.7	0.9	0.4	0.5	0.31	0.7

Table 1 continued

Chemical composition	Commercial granites						
	Grigio Malaga Sa15[a]	Rosa Beta	Grigio Perla	Ghiandone	Rosa Cinzia	Bianco Sardo Sa22c[a]	San Giacomo
Dy	3.12	4	5.8	2.5	2.7	1.74	3.7
Ho	0.59	0.8	1.2	0.5	0.5	0.34	0.7
Er	1.62	2.2	3.6	1.5	1.5	0.97	2.2
Tm	0.21	0.34	0.61	0.25	0.23	0.14	0.32
Yb	1.51	2.3	4.1	1.7	1.6	0.95	2.1
Lu	0.24	0.37	0.7	0.32	0.29	0.18	0.33
Hf	4	6.7	3.3	3	2.8	3	7.6
Ta	–	1.4	1.5	1	0.7	–	0.5
W	–	<1	<1	<1	<1	–	<1
Tl	–	0.5	1	0.6	0.8	–	0.5
Pb	–	21	26	18	21	–	27
Bi	–	< 0.4	< 0.4	< 0.4	< 0.4	–	<0.4
Th	15	12.9	17	14.4	15.6	11	15.1
U	2	5.2	3.1	4	3.6	2	2.6

[a] Data taken from (Barbey et al. 2008)

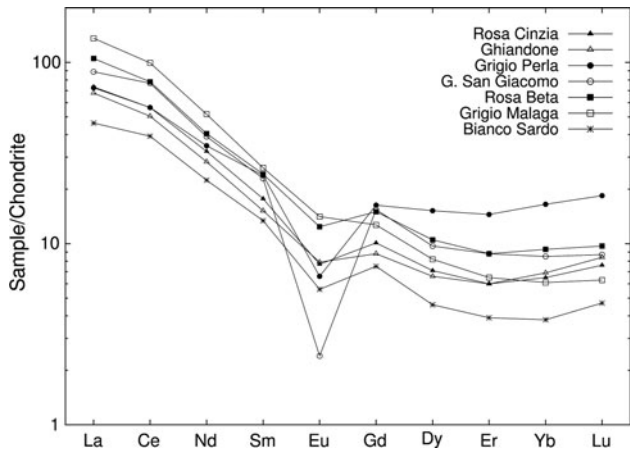

Fig. 3 Chondrite normalized REE patterns of the seven granite dimension stones analyzed

were chosen, far from the sides of the outcrop and from man-made constructions. The portable NaI(Tl) detector was placed on bare rocks with no soil cover or vegetation. The measurements were never performed immediately after rainfalls and since the detector was placed on bare rocks the interference of moisture was considered negligible. The ^{238}U and ^{232}Th activity concentrations were calculated assuming secular equilibrium in the decay series.

The activity concentrations of ^{40}K, ^{238}U and ^{232}Th obtained from in situ surveys were compared with those measured in individual samples of each commercial granite using inductively coupled plasma mass spectrometry (ICP-MS) and HPGe spectrometry (Table 2). The elemental composition measurements were performed at Activation Laboratories Ltd. using a Perkin Elmer SCIEX ELAN 9000 ICP/MS with a combination of analysis packages Code 4B (lithium metaborate/tetraborate fusion ICP whole rock) and Code 4B2 (trace element ICP-MS), in which the fused sample is diluted and analyzed using ICP-MS. The detection limits of these methods for K_2O, U and Th were 0.01 % (2.6 Bq/kg), 0.1 μg/g (1.2 Bq/kg) and 0.1 μg/g (0.4 Bq/kg), respectively. The ICP-MS method permits not only to crosscheck in situ measurements, but it also provides information on the major and trace element composition necessary for the geochemical characterization of different granites (see Sect. 3).

The activity concentrations were measured on a 180 cm^3 sample using the MCA_Rad system (Xhixha et al. 2013). The fully automatic spectrometer consists of two 60 % relative efficiency coaxial p-type HPGe gamma-ray detectors, with an energy resolution of ~1.9 keV at 1332.5 keV (^{60}Co). The absolute full energy peak efficiency of the MCA_Rad is calibrated using certified standard point sources (^{152}Eu and ^{56}Co). The overall uncertainty in the efficiency calibration is estimated to be <5 %.

Results and discussion

Statistical analysis

The latter measurements were used to determine the radiological hazard of 7 types of commercial granites. The distributions of the ^{40}K, ^{238}U and ^{232}Th activity concentration of these two classes of data are reported in Figs. 4,

Table 2 Median values of the log-normal distributions of ^{40}K, ^{238}U and ^{232}Th activity concentration with 1σ asymmetrical uncertainty, based on 21 in situ measurements (NaI:Tl). For each commercial granite, a measurement was performed with HPGe detectors and ICP-MS. In the fourth row are reported data published in the literature (in brackets the number of samples). The activity concentration index (ACI) and default dose categories are indicated in the last two columns

Commercial brand	Quarries/HPGe analysis/bibliography	^{40}K (Bq/kg)	^{238}U (Bq/kg)	^{232}Th (Bq/kg)	ACI	Category
Rosa Beta	NaI:Tl (20 quarries)	$1{,}144^{+126}_{-114}$	$42.3^{+7.7}_{-6.6}$	$55.0^{+6.8}_{-5.9}$	$0.78^{+0.06}_{-0.06}$	A1
	HPGe	1059 ± 19	37.4 ± 2.0	55.1 ± 2.9		A2
	ICP-MS[a]	1,020	64	52		
	(Tzortzis et al. 2003; Al-Saleh and Al-Berzan 2007; Aydarous et al. 2010; Carrera et al. 1996; SR 2012) (9 data)	897–1,221	18.2–45.2	32.0–69.0		
Ghiandone	NaI:Tl (20 quarries)	$1{,}092^{+215}_{-181}$	$56.3^{+14.1}_{-11.4}$	$68.9^{+11.2}_{-9.6}$	$0.88^{+0.11}_{-0.09}$	A1/B1
	HPGe	953 ± 21	49.6 ± 2.4	50.8 ± 3.1		A2
	ICP-MS	840	49	58		
	(Tzortzis et al. 2003; SR 2012) (5 data)	736–1,047	33.3–57.0	59.1–89.0		
G. San Giacomo	NaI:Tl (13 quarries)	$1{,}335^{+142}_{-128}$	$50.1^{+15.7}_{-11.9}$	$61.9^{+10.1}_{-8.7}$	$0.91^{+0.10}_{-0.08}$	A1/B1
	HPGe	1284 ± 25	53.2 ± 2.6	55.0 ± 3.6		A2
	ICP-MS	1,257	28	62		
	(SR 2012) (2 data)	919–1,019	19.8–58.6	47.5–58.0		
Rosa Cinzia	NaI:Tl (2 quarries)	$1{,}313^{+66}_{-63}$	$56.0^{+7.2}_{-6.5}$	$69.4^{+3.5}_{-3.3}$	$0.95^{+0.04}_{-0.04}$	A1/B1
	HPGe	1,296 ± 25	46.2 ± 2.4	60.2 ± 3.5		A2
	ICP-MS	1,205	44	63		
	(SR 2012) (1 data)	1,023	34.0	56.1		
Grigio Malaga	NaI:Tl (8 quarries)	848^{+130}_{-113}	$34.5^{+5.0}_{-4.3}$	$61.1^{+5.8}_{-5.3}$	$0.66^{+0.05}_{-0.05}$	A1
	HPGe	711 ± 18	29.2 ± 2.0	52.8 ± 3.2		A2
	ICP-MS (Barbey et al. 2008)	970	25	61		
	(SR 2012) (1 data)	748	22.9	51.2		
Grigio Perla	NaI:Tl (7 quarries)	$1{,}222^{+165}_{-145}$	$39.1^{+5.6}_{-4.9}$	$60.6^{+6.0}_{-5.5}$	$0.81^{+0.06}_{-0.06}$	A1
	HPGe	1,270 ± 25	52.3 ± 2.6	61.0 ± 3.6		A2
	ICP-MS	1,140	38	69		
	(Carrera et al.1996; SR 2012) (2 data)	1,039–1,208	33.7–37.0	45.3–58.0		
Bianco Sardo	NaI:Tl (3 quarries)	$1{,}269^{+66}_{-63}$	$44.8^{+7.6}_{-6.5}$	$51.6^{+7.8}_{-6.8}$	$0.82^{+0.05}_{-0.05}$	A1
	HPGe	1,355 ± 25	40.8 ± 2.3	50.5 ± 3.1		A2
	ICP-MS (Barbey et al. 2008)	1,255	25	45		
	(Carrera et al. 1996) (1 data)	1,137	48	95		

[a] Conservatively, an accuracy of 10 % for ICP-MS results was assumed

5, and 6. The variances of the commercial granite data are slightly smaller than those of the data collected at scattered locations on outcrops of the C-SB. Both classes generally have non-normal distributions. The distribution of ^{40}K in non-commercial (commercial) granites shows negative skewness of −1.1 (−0.7), while the distributions of ^{238}U and ^{232}Th show positive skewness of 1.3 (1.2) and 0.8 (0.1), respectively. The distributions are well fitted with a log-normal probability function (Ahrens 1954) (as reported in footnotes in Fig. 4, 5, and 6 the reduced χ^2 is <2 with exception to the case of ^{40}K in non-commercial C-SB granites where it is 4.3), which was used to calculate the asymmetrical (geometric) standard deviation (Table 2).

These results are used to calculate the absorbed dose rate in outdoor air and the ACI, when the combined asymmetric uncertainties were estimated by Monte Carlo method (Huang et al. 2012; JCGM 2008). In particular, 10^5 pseudo-random samples for each input (^{40}K, ^{238}U and ^{232}Th) are generated according to the specific distribution parameters (median and 1σ uncertainty). The distributions of the absorbed dose rate and the ACI were estimated by repeating the process over a cycle of iterations and the median and combined asymmetric uncertainties are evaluated. This improved analysis accounts for the non-normal distribution of elements in igneous rocks. By adopting a log-normal distribution as the universal form of the

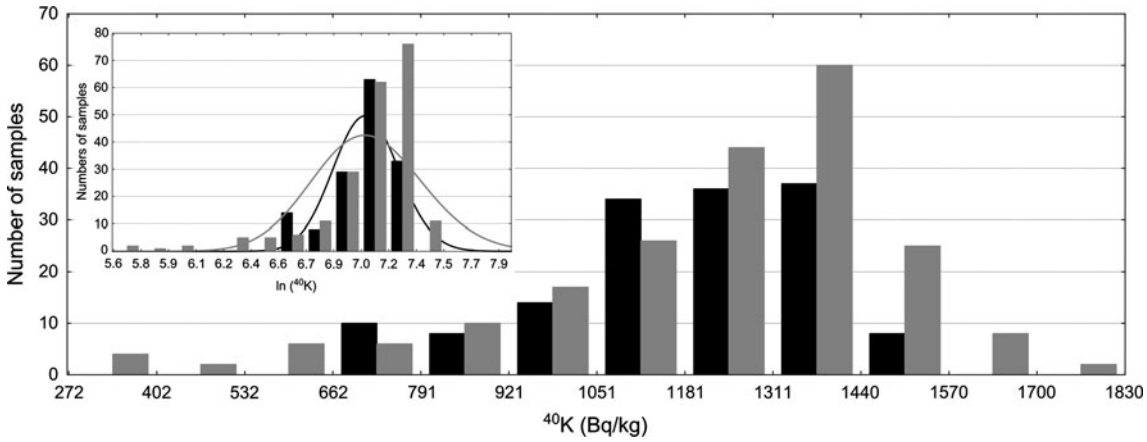

Fig. 4 Distribution of the activity concentration of ^{40}K in Bq/kg. The 210 measures of non-commercial C-SB granitic rocks (in *gray*), and 147 measures of commercial granitic rocks (in *black*) are fitted with log-normal distributions showing, respectively, a reduced χ^2 of 4.3 and 1.8

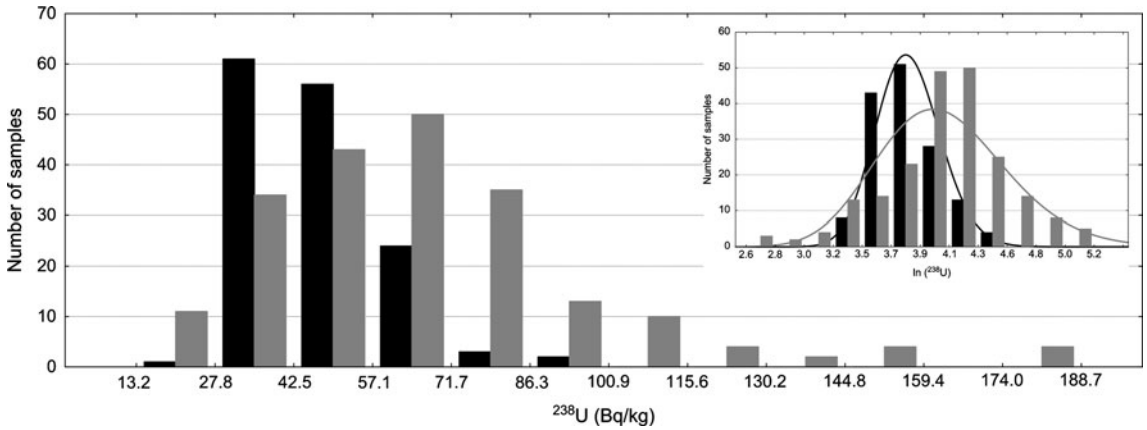

Fig. 5 Distribution of the activity concentration of ^{238}U in Bq/kg. The 210 measures of non-commercial C-SB granitic rocks (in *gray*), and 147 measures of commercial granitic rocks (in *black*) are fitted with log-normal distributions showing, respectively, a reduced χ^2 of 1.6 and 0.7

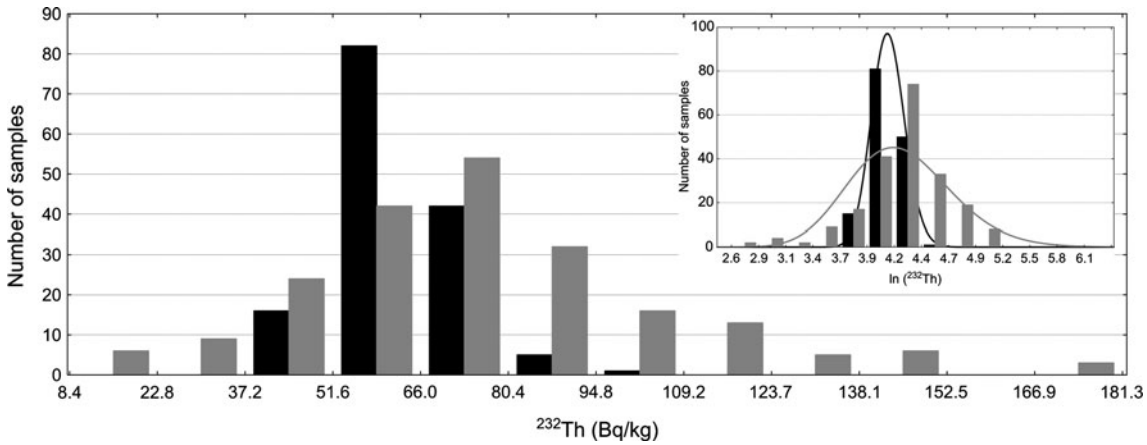

Fig. 6 Distribution of the activity concentration of ^{232}Th in Bq/kg. The 210 measures of non-commercial C-SB granitic rocks (in *gray*), and 147 measures of commercial granitic rocks (in *black*) are fitted with log-normal distributions showing, respectively, a reduced χ^2 of 1.6 and 0.8

abundance distribution, the incidence of high values in the tails of the distribution is increased. Based on the statistical meaning of a 1σ uncertainty, we are able to quantify the probability of exceeding a given absorbed dose rate and/or ACI.

Radiological characterization of the C-SB granitic rocks

The radioactivity concentrations of the C-SB granitic plutons are generally higher than those typical for the upper continental crust (Rudnick and Gao 2003). The activity concentrations of ^{40}K, ^{238}U and ^{232}Th (at 1σ uncertainty) are $1{,}177^{+408}_{-304}$, 60^{+36}_{-23} and 69^{+38}_{-25} Bq/kg, respectively. The abundances of ^{238}U and ^{232}Th are comparable to those in the upper portion of the continental crust at the 1σ level, while the ^{40}K content is $\sim 2\sigma$ higher. The relatively high concentration of radioelements in the C-SB crust could be related to the origin of the extensive HT-LP province established in the Variscan belt during the Carboniferous–Permian transition, as discussed in (Lexa et al. 2011; Schulmann et al. 2008). The wide spread of the measurements made on outcrops in the Sardinian sector of the Batholith is a consequence of a coalescence of many calc-alkaline plutons (see Sect. 2). The Sardinian Batholith crust has a lower average abundance ratio of K/U and Th/U values of 7.8×10^3 and 3.5, respectively.

The absorbed dose rate in air from external gamma radiation at 1 m above ground level due to the presence of natural radionuclides in measured outcrops is calculated as (UNSCEAR 2000)

$$D\ (\text{nGy h}^{-1}) = 0.0417\ C_{\text{K}} + 0.462\ C_{\text{U}} + 0.604\ C_{\text{Th}},$$

where C_{K}, C_{U}, C_{Th} are the activity concentrations (in Bq/kg) of ^{40}K, ^{238}U (^{226}Ra) and ^{232}Th. In the C-SB, the outdoor absorbed dose rate at 1σ uncertainty is 124^{+33}_{-26} nGy/h (the maximum and minimum calculated values are 28 and 256 nGy/h). This dose is 3σ higher than the population-weighted average absorbed dose rate in outdoor air from terrestrial gamma radiation (60 nGy/h). However, only 3.3 % of our measurements exceed the upper limit of the worldwide typical range of variability of 10–200 nGy/h (UNSCEAR 2000).

The radiological hazard is evaluated using the annual effective dose rate (expressed in mSv/y). Adopting a conversion factor of 0.7 (Sv/Gy) (UNSCEAR 2000), which accounts for the dose biological effectiveness in causing damage to human tissue and an outdoor time occupancy factor of 20 %, was calculated the annual effective dose rate of the population living in the C-SB area. The obtained annual outdoor effective dose rate of $0.15^{+0.04}_{-0.03}$ mSv/y is 3σ higher than the worldwide annual effective dose value of 0.07 mSv/y reported by UNSCEAR (2000).

For each commercial granite, a measurement was performed with HPGe detectors and ICP-MS. In the fourth row are reported data published in the literature (in brackets the number of samples). The ACI (ACI) and default dose categories are indicated in the last two columns.

ACI of commercial granites

The radiological characterization of the seven commercial granites is reported in Table 2. The abundances of ^{40}K and ^{232}Th exceed those in the upper continental crust by more than 1σ for all of the granites except *Grigio Malaga* and *Bianco Sardo*. The ^{238}U abundance is comparable to that in the upper continental crust at the 1σ level for all except *Ghiandone* and *Rosa Cinzia*. However, the spreads of the distributions are narrower than those for the C-SB pluton outcrops: for ^{40}K and ^{232}Th, 68.3 % of the data lie within 12 % of the median value. The higher variance ($< \sigma > \sim 20$ %) of the ^{238}U measurements is comparable to the systematic uncertainty of the NaI(Tl) detector. In general, the distributions of the *Rosa Cinzia* and *Bianco Sardo* are narrower, and these considering the number of quarries investigated, respectively, 2 and 3, is an evidence on the reliability of the measures representing the variability of commercial granites quarried in C-SB area.

The radiological hazard of rocks used as building materials can be evaluated using the ACI (ACI), proposed by EC (2011):

$$\text{ACI} = \frac{C_{\text{Ra}}}{300} + \frac{C_{\text{Th}}}{200} + \frac{C_{\text{K}}}{3{,}000},$$

where C_{Ra}, C_{Th} and C_{K} are the activity concentrations in Bq/kg for ^{226}Ra (equivalent to ^{238}U under secular equilibrium conditions), ^{232}Th and ^{40}K, respectively. Following EC (2011), the radiological hazard is classified into four categories. The first category of materials is appropriate for use in bulk quantities, while the second category of materials is limited to superficial or other restricted use (Table 3). The contribution to the ACI index of the median radioactivity content for potassium, uranium and thorium is shown in Fig. 7. It shows that ~ 50 % of the ACI index comes from ^{40}K.

The ACI varies from $0.66^{+0.05}_{-0.05}$ for *Grigio Malaga* to $0.95^{+0.04}_{-0.04}$ for *Rosa Cinzia*. Because they have ACIs < 6 within the reported standard deviation, these rocks are categorized as A2 (suitable for being used as surface materials without restriction). The ACIs of *Rosa Beta*, *Grigio Malaga*, *Grigio Perla* and *Bianco Sardo* are more than 2σ below unity and, therefore, these materials can be classified as A1 (suitable for being used as bulk materials without restriction). However, *Rosa Cinzia*, *Giallo san Giacomo* and *Ghiandone* have ACIs within 1σ of unity. In

Table 3 Categories based on the default dose according to the ACI (ACI) criteria defined in EC (2011)

Category (corresponding default dose)	Type 1 Materials used in bulk amounts e.g. concrete, bricks etc.	Type 2 superficial and other materials with restricted use e.g. tiles, boards etc.
A ($\leq$1 mSv/y)	For ACI $\leq$ 1 category **A1**	For ACI $\leq$ 6 category **A2**
B (>1 mSv/y)	For ACI > 1 category **B1**	For ACI > 6 category **B2**

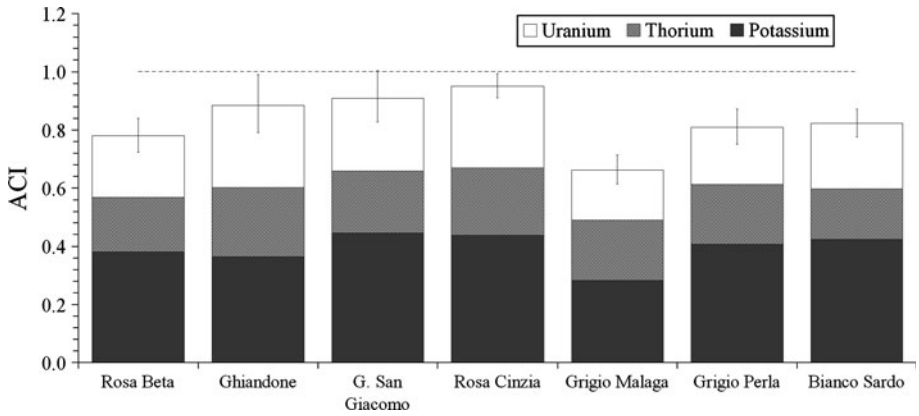

Fig. 7 The ACI (ACI) calculated for each commercial granite using the median values for ^{40}K, ^{238}U and ^{232}Th

these cases, it is reported the classification A1/B1 (Table 2) to emphasize a potential radiological hazard in bulk utilization of these commercial granites, and recommend further ad hoc controls.

The activity concentrations measured with NaI:Tl and HPGe spectrometry are comparable at the 1σ level; however, the data collected in situ are more robust since they are supported by more observations. Although some of the ICP-MS data are 2σ away (only for *Bianco Sardo* was found a discrepancy at 3σ for ^{238}U activity concentration) from the median of the in situ investigations, there is general agreement between the ^{40}K, ^{238}U and ^{232}Th abundances measured using the three different methods. However, the laboratory measurements are based on the assumption that the samples are representative of the entire dimension stone. This hypothesis is weak, and may increase the discrepancies with respect to the in situ data. In the case of the granitic rocks of the C-SB, the in situ measurements provide a suitable method of investigation, as indicated by previously published data (Table 2).

Summary and conclusions

An extensive in situ survey was performed for the first time in the C-SB area using a portable NaI(Tl) scintillation detector for the determination of the radioactivity concentration of ^{40}K, ^{238}U and ^{232}Th on 210 intrusive granite outcrops. Moreover, the radioactivity content of the main seven commercial granites quarried in 73 extractive sites in this area was investigated by means of 147 in situ measurements. This approach made it possible to collect a large statistics of samples while minimizing time and costs, and optimizing the spectral analysis through FSA-NNLS. The large number of measurements permitted to perform an accurate analysis of the data based on assumed log-normal distributions of the radioelements. The propagation of asymmetrical uncertainties was treated using a Monte Carlo method instead of assuming Gaussian errors, increasing the quality of the radiological characterization of the rocks.

The in situ measurements on granitoid outcrops of the C-SB showed activity concentrations of $1{,}177^{+408}_{-304}$, 60^{+36}_{-23} and 69^{+38}_{-25} Bq/kg for ^{40}K, ^{226}Ra (^{238}U) and ^{232}Th, respectively. These data are found to be comparable at the 1σ level to those in the upper continental crust for uranium and thorium, whereas the potassium content is $\sim$2σ higher. These results were used to assess the outdoor absorbed dose rate, which is 124^{+33}_{-26} nGy/h (ranging between 28 and 256 nGy/h), and exceeding the reported UNSCEAR (2000) population-weighted average absorbed dose rate (60 nGy/h) by more than 3σ. However, only 3.3 % of our measurements exceed the upper limit of the worldwide typical range of variability of 10–200 nGy/h. The corresponding annual outdoor effective dose rate for the population living in the C-SB area is calculated to be $0.15^{+0.04}_{-0.03}$ mSv/y.

The ^{40}K, ^{238}U and ^{232}Th activity concentrations of commercial granites measured in 73 quarries show good agreement (at 2σ level) compared to data from representative samples using ICP-MS and HPGe spectrometry. The ACI of the seven traded varieties was found to range between $0.66^{+0.05}_{-0.05}$ for *Grigio Malaga* and $0.95^{+0.04}_{-0.04}$ for

Rosa Cinzia. All of these granites are categorized with 3σ confidence as A2 material, permitting their utilization as superficial materials without restrictions. *Rosa Beta*, *Grigio Malaga*, *Grigio Perla* and *Bianco Sardo* are categorized with 2σ confidence as A1 materials, and may, therefore, also be used in bulk quantities without restriction. However, *Ghiandone*, *Giallo San Giacomo* and *Rosa Cinzia* have activity concentration indices within 1σ of the limiting value, and further ad hoc controls are, therefore, recommended for their utilization in bulk quantities.

Acknowledgments The authors are grateful to G. P. Bezzon, C. Broggini, G. P. Buso, A. Caciolli, L. Carmignani, T. Colonna, S. De Bianchi, G. Fiorentini, M. Gambaccini, Y. Huang, W. F. McDonough, R. Menegazzo, L. Mou, R. L. Rudnick, M. Shyti and A. Zanon for useful comments and discussions. This work was funded by the Banco di Sardegna Foundation (G. Oggiano grant) and Sardinia Government grant L.R. 7/2007—no CRP2_104 (L. Casini and S. Cuccuru) and was partially supported by National Institute of Nuclear Physics, INFN (Italy).

References

Ahrens LH (1954) The lognormal distributions of the elements. (A fundamental law of geochemistry and its subsidiary). Geochim Cosmochim Acta 5:49–73

Al-Saleh FS, Al-Berzan B (2007) Measurements of natural radioactivity in some kinds of marble and granite used in Riyadh region. J Nucl Rad Phys 2:25–36

Anjos RM, Veiga R, Soares T, Santos AMA, Aguiar JG, Frascá MHBO, Brage JAP, Uzêda D, Mangia L, Facure A, Mosquera B, Carvalho C, Gomes PRS (2005) Natural radionuclide distribution in Brazilian commercial granites. Radiat Meas 39:245–253

Aydarous ASh, Zeghib S, Al-Dughmah M (2010) Measurements of natural radioactivity and the resulting radiation doses from commercial granites. Radiat Prot Dosim 142:363–368

Barbey P, Gasquet D, Pin C, Bourgeix AL (2008) Igneous banding, schlieren and mafic enclaves in calc-alkaline granites: the Budduso pluton (Sardinia). Lithos 104:147–163

Bralia A, Ghezzo C, Guasparri G, Sabatini G (1981) Aspetti genetici del batolite sardo-corso. Rend Soc Ital Miner Petrol 38:701–764

Caciolli A, Baldoncini M, Bezzon GP, Broggini C, Buso GP, Callegari I, Colonna T, Fiorentini G, Guastaldi E, Mantovani F, Massa G, Menegazzo R, Mou L, Rossi Alvarez C, Shyti M, Xhixha G, Zanon A (2012) A new FSA approach for in situ γ ray spectroscopy. Sci Total Environ 414:639–645

Carrera G, Garavaglia M, Magnoni S, Valli G, Vecchi R (1996) Natural radioactivity and radon exhalation in stony materials. J Environ Radioactiv 34:149–159

Casini L (2012) A MATLAB-derived software (geothermMOD1.2) for one-dimensional thermal modeling, and its application to the Corsica-Sardinia batholith. Comput Geosci 45:82–86

Casini L, Cuccuru S, Maino M, Oggiano G, Tiepolo M (2012) Emplacement of the Arzachena Pluton (Corsica-Sardinia Batholith) and the geodynamics of incoming Pangaea. Tectonophysics 544:31–49

Cherchi GP (2005) Prospezione e caratterizzazione di rocce granitoidi della Sardegna settentrionale: indicazioni per l'ottimizzazione del processo estrattivo e della mitigazione degli impatti. PhD. Thesis (in Italian), University of Sassari

Cocherie A, Fouillac R, Vidal AM (1994) Crust and mantle contributions to granite genesis—an example from the Variscan batholith of Corsica, France, studied by trace element and Nd–Sr–O-isotope systematics. Chem Geology 115:173–211

Cocherie A, Rossi P, Fanning CM, Guerrot C (2005) Comparative use of TIMS and SHRIMP for U-Pb zircon dating of A-type granites and mafic tholeiitic layered complexes and dykes from the Corsican Batholith (France). Lithos 82:185–219

Cuccuru S, Gamboni A, Casini L (2011) The Mt. Mazzolu quarry: a new mineralogic locality Plinius 37:304

Cuccuru S, Casini L, Oggiano G, Cherchi GP (2012) Can weathering improve the toughness of a fractured rock? A case study using the San Giacomo Granite. Bull Eng Geol Environ 71(3):557–567

European Commission (EC) (2011) Draft presented under Article 31 Euratom Treaty for the opinion of the European Economic and Social Committee: laying down basic safety standards for protection against the dangers arising from exposure to ionising radiation. COM(2011) 593, Brussels. http://ec.europa.eu/energy/nuclear/radiation_protection/doc/com_2011_0593.pdf. Accessed 26 Oct 2011

Faure M, Cocherie A, Bé Mézème E, Charles N, Rossi P (2010) Middle carboniferous crustal melting in the Variscan Belt: new insights from U–Th–Pbtot monazite and U–Pb zircon ages of the Montagne Noire Axial Zone (southern French Massif Central). Gondwana Res 18(4):653–673

Ferrè EC, Leake BE (2001) Geodynamic significance of early orogenic high-K crustal and mantle melts: example of the Corsica-Sardinia Batholith. Lithos 59:47–67

Gaggero L, Oggiano G, Buzzi L, Slejko F, Cortesogno L (2007) Post-Variscan mafic dykes from the late orogenic collapse to the Tethyan rift: evidence from Sardinia. Ofioliti 32:15–37

Gamboni A, Gamboni T (2006) Gallura, tesori nel granito, i minerali delle pegmatiti granitiche. Webber, Sassari

Ghezzo C, Orsini J-B (1982) Lineamenti strutturali e composizionali del batolite ercinico sardo corso in Sardegna. In: Guida alla geologia del Paleozoico Sardo, Soc Geol Ita, Roma, pp 88–102

Huang Y, McDonough WF, Mantovani F (2012) Propagation of uncertainties in geochemistry by Monte Carlo simulation. Chem Geol (Submitted)

Joint Committee for Guides in Metrology (JCGM) (2008) Evaluation of measurement data—supplement 1 to the "guide to the expression of uncertainty in measurement"—propagation of distributions using a Monte Carlo method (1st edn). JCGM 101, p 90

Lexa O, Schulmann K, Janoušek V, Stipskà P, Guy A, Racek M (2011) Heat sources and trigger mechanisms of exhumation of HP granulites in Variscan orogenic root. J Metamorphic Geol 29:79–102

Oggiano G, Cherchi G P, Aversano A, Di Pisa A, Ulzega A, Orrù P, Pintus C (2005) Note illustrative della Carta Geologica d'Italia, Arzachena

Oggiano G, Casini L, Rossi P H, Mameli P (2007) Long lived dextral strike-slip tectonics in the southern Variscan Belt: evidence from two syn-kynematic intrusions in north Sardinia, vol 2. In: Geologie de la France, Meeting on Mechanics of Variscan Orogeny: a modern view on orogenic research, Orleans, Sept. 13–15, p 141

Paquette J-L, Ménot R-P, Pin C, Orsini J-B (2003) Episodic and short-lived granitic pulses in a post-collisional setting: evidence from precise U-Pb zircon dating through a crustal cross-section in Corsica. Chem Geol 198:1–20

Poggi D, Lazzarini L (2005) Il granito sardo: cave e cavatura. Usi, diffusione e aspetti archeometrici. Marmora 1:49–68

Regione Autonoma della Sardegna (RAS) (2007) Piano Regionale delle Attività Estrattive: riepilogo dei principali dati, Cagliari

Renna MR, Tribuzio R, Tiepolo M (2006) Interaction between basic and acid magmas during the latest stages of the post-collisional Variscan evolution: clues from the gabbro–granite association of Ota (Corsica–Sardinia batholith). Lithos 90:92–110

Rogers JJW, Ragland PC (1961) Variation of thorium and uranium in selected granitic rocks. Geochim Cosmochim Acta 25:99–109

Rossi P, Oggiano G, Cocherie A (2009) A restored section of the "southern Variscan realm" across the Corsica-Sardinia microcontinent. Comp Rend Geosci 341:224–238

Rudnick R L, Gao S (2003) Composition of the Continental Crust, vol 3. In: Holland H D, Turekian KK (eds) Treatise on geochemistry: meteorites, comets and planets, vol 1, Elsevier Ltd., Oxford, pp 59–659

Salas HT, Nalini HA Jr, Mendes JC (2006) Radioactivity dosage evaluation of Brazilian ornamental granitic rocks based on chemical data, with mineralogical and lithological characterization. Environ Geol 49:520–526

Sardegna Ricerche (SR) (2012) Progetto Cluster "radioattività nei materiali da costruzione". http://www.sardegnaricerche.it/documenti/13_116_20110114161302.pdf. Accessed 1 Aug 2012

Schulmann K, Lexa O, Štípskà P, Racek M, Tahčmanovà L, Konopàsek J, Edel J-B, Peschler A, Lehmann J (2008) Vertical extrusion and horizontal channel flow of orogenic lower crust: key exhumation mechanisms in large hot orogens? J Metamorphic Geol 26:273–297

Tzortzis M, Tsertos H, Christofides S, Christodoulides G (2003) Gamma radiation measurements and dose rates in commercially-used natural tiling rocks (granites). J Environ Radioactiv 70:223–235

UNI (Ente Nazionale Italiano di Unificazione). Natural stone—denomination criteria. UNI-EN 12440:2008

United Nations Scientific Committee on the Effects of Atomic Radiation (UNSCEAR) (2000) Exposures from Natural Radiation Sources. UN, New York

Whitfield JM, Rogers JJW, Adams JAS (1959) The relationship between the petrology and the thorium and uranium contents of some granitic rocks. Geochim Cosmochim Acta 17:248–271

Xhixha G, Bezzon GP, Broggini C, Buso GP, Caciolli A, Callegari I, De Bianchi S, Fiorentini G, Guastaldi E, Mantovani F, Massa G, Menegazzo R, Mou L, Pasquini A, Rossi Alvarez C, Shyti M, Xhixha Kaçeli M (2013) The worldwide NORM production and a fully automated gamma-ray spectrometer for their characterization. J Radioanal Nucl Chem 295:445–457